BERNARD

A PROJECTILE PENETRATION THEORY FOR LAYERED TARGETS

ROBERT S. BERNARD
U. S. ARMY ENGINEER WATERWAYS EXPERIMENT STATION
VICKSBURG, MISSISSIPPI 39180

DNA-NWE-SB-211

INTRODUCTION

Projectile penetration ~~has been~~ was studied by military engineers since ancient times, but the analytical investigation of this phenomenon was not undertaken until the eighteenth century. Robins (1), Euler (2), and Poncelet (3) developed the first empirical equations describing the axial force which opposes the motion of a rigid projectile as it passes through a deformable solid target. Experimental data consisting of impact velocity and final depth of penetration were used to estimate the coefficients in the relation between axial force and projectile velocity. However, these coefficients were not specified in terms of standard material properties, and so they were applicable only for the particular targets for which they were determined. → next page

Since the mid-twentieth century, the availability of high-speed digital computers has made it possible to analyze the projectile/target interaction by means of two-dimensional finite-difference techniques. The constitutive relations for both the target and the projectile can be accurately specified, and many of the details in the penetration process can be realistically simulated. Analyses of this kind are valuable because of the detailed information which they provide, but they are usually too costly and cumbersome for large scale parameter studies.

In recent years, significant progress has been made toward the development of a simple relation between penetration resistance and fundamental target properties such as density and compressive

strength. Bishop, Hill, and Mott (4) analyzed the quasistatic expansion of spherical and cylindrical cavities in metals and observed a correlation between the resistance to cavity expansion and the resistance to indentation by a rigid static punch. Goodier (5) used an analogy with the dynamic expansion of spherical cavities in metals to develop a penetration theory for rigid spherical projectiles. In the present work, the quasistatic expansion of a spherical cavity in a concentrically layered medium will be analyzed in order to obtain an approximation for the radial stress at the surface of a slowly expanding spherical cavity in a vertically layered medium with a plane interface. This approximation will then be used to construct a simple equation of motion for a rigid cylindrical projectile (with a conical or ogival nose shape) which penetrates a layered target.

SPHERICAL CAVITY EXPANSION IN A CONCENTRICALLY LAYERED MEDIUM

Consider a slowly expanding spherical cavity surrounded by an infinite medium composed of two distinct concentric layers (Figure 1). The materials surrounding the cavity exhibit elastic-plastic behavior without volume change (Figure 2). The geometry is spherically symmetric and the material equation of equilibrium is

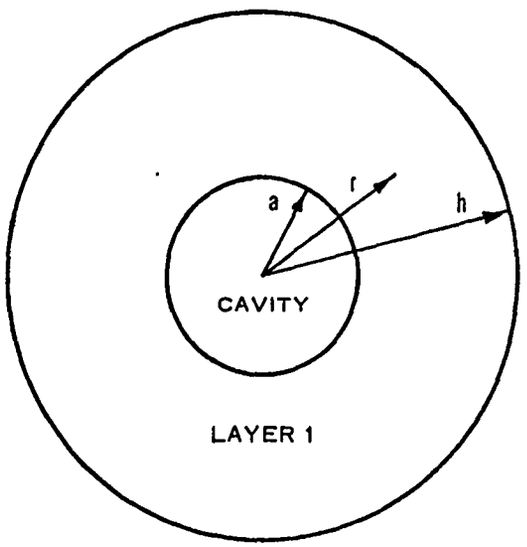

Figure 1. Slowly expanding spherical cavity in a concentrically layered medium

$$\frac{d\sigma_r}{dr} + \frac{2}{r}(\sigma_r - \sigma_\theta) = 0 \qquad (1)$$

where r is the radial coordinate and σ_r and σ_θ are respectively the radial and circumferential components of stress. (Compressive stress and strain are taken to be positive.) The stress-strain relation for the material in the elastic state is

$$\sigma_r - \sigma_\theta = \frac{2}{3} E(\varepsilon_r - \varepsilon_\theta) \qquad (2)$$

and in the plastic state it is

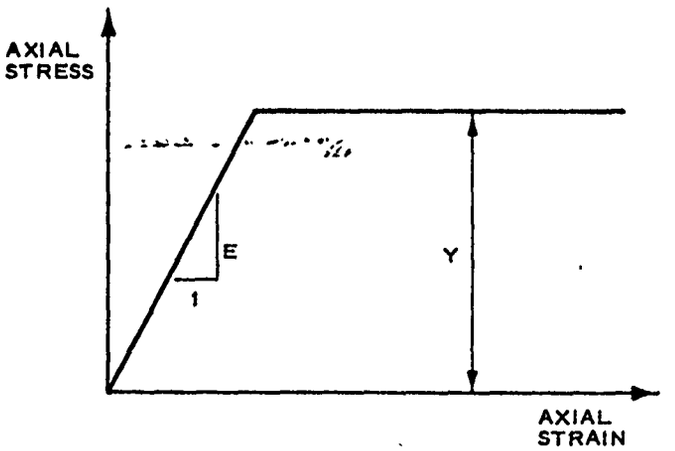

Figure 2. Material response to uniaxial stress

$$\sigma_r - \sigma_\theta = Y \tag{3}$$

where E is the elastic modulus, Y is the compressive strength, and ε_r and ε_θ are respectively the radial and circumferential strains. Both materials are incompressible, and the relation between ε_r and ε_θ is

$$\varepsilon_r + 2\varepsilon_\theta = 0 \tag{4}$$

Equations 2 and 4 are now combined so that the stress-strain relation in the elastic state becomes

$$\sigma_r - \sigma_\theta = -2E\varepsilon_\theta \tag{5}$$

The circumferential strain at any radial position is given by

$$\varepsilon_\theta = -\ln \frac{r}{r_o} \tag{6}$$

where r_o is the initial radial position of a material particle which has been displaced to position r. Assuming that the spherical cavity expands from a small initial radius a_o to an instantaneous radius $a >> a_o$, the principle of conservation of mass requires that

$$r^3 - r_o^3 = a^3 - a_o^3 \approx a^3 \tag{7}$$

When Equation 7 is rearranged, it follows that

$$\frac{r^3}{r_o^3} \approx \left(1 - \frac{a^3}{r^3}\right)^{-1} \tag{8}$$

and the expression for the circumferential strain becomes

$$\varepsilon_\theta \approx \frac{1}{3} \ln \left(1 - \frac{a^3}{r^3}\right) \tag{9}$$

Restricting attention to small strains in the elastic state, Equation 9 is further approximated by

$$\varepsilon_\theta \approx - \frac{1}{3} \frac{a^3}{r^3} \tag{10}$$

and the stress-strain relation in the elastic state now becomes

$$\sigma_r - \sigma_\theta \approx \frac{2}{3} E \frac{a^3}{r^3} \tag{11}$$

Combining Equation 1 alternately with Equations 3 and 11, the material equation of equilibrium in the plastic state is

$$\frac{d\sigma_r}{dr} = - \frac{2}{r} Y \tag{12}$$

and in the elastic state it is

$$\frac{d\sigma_r}{dr} = - \frac{4}{3} E \frac{a^3}{r^4} \tag{13}$$

Each material layer may contain distinct elastic and plastic regions (Figure 3) which are separated by spherical plastic "fronts" located at $r = b$ and $r = k$ in layers 1 and 2, respectively. It is obvious from Figure 3 that $b \leq h$ since the plastic region in layer 1 cannot extend beyond the location of the layer interface at $r = h$. Similarly, it follows that $k \geq h$ in layer 2. Evaluating Equations 12 and 13 at $r = b$ and $r = k$ and equating the right-hand sides at each of these locations, then it is found that

$$b = a \left(\frac{2E_1}{3Y_1}\right)^{1/3} , \quad \frac{2E_1}{3Y_1} \leq \frac{h^3}{a^3} \tag{14}$$

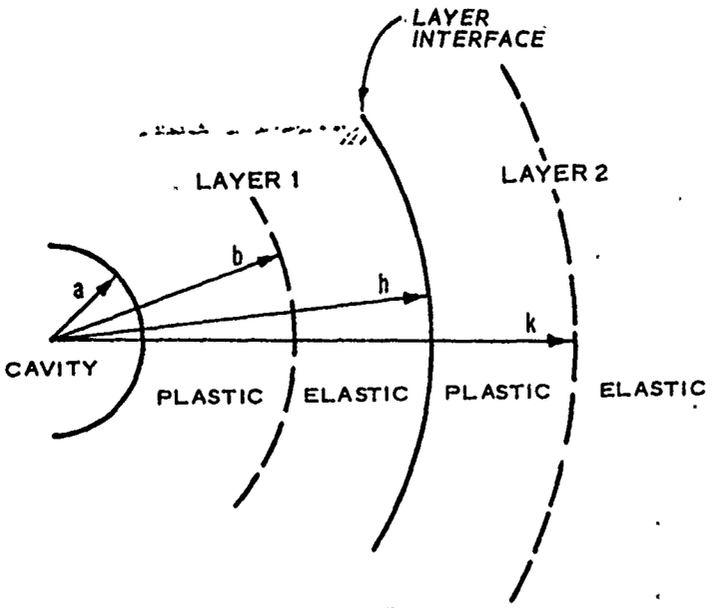

Figure 3. Location of concentric elastic and plastic regions surrounding cavity

$$b = h \;, \quad \frac{2E_1}{3Y_1} \geq \frac{h^3}{a^3} \tag{15}$$

and that

$$k = h \;, \quad \frac{2E_2}{3Y_2} \leq \frac{h^3}{a^3} \tag{16}$$

$$k = a\left(\frac{2E_2}{3Y_2}\right)^{1/3} \;, \quad \frac{2E_2}{3Y_2} \geq \frac{h^3}{a^3} \tag{17}$$

where the subscripts 1 and 2 indicate the evaluation of quantities in layers 1 and 2, respectively. Denoting the initial radial position of the layer interface by h_o and evaluating Equation 7 at $r = h$, the relation between the cavity radius and the position of the layer interface becomes

$$h^3 \approx h_o^3 + a^3 \tag{18}$$

The positions of the layer interface and the plastic

fronts are now completely specified in terms of the cavity radius, and Equations 12 and 13 can be integrated to determine the radial stress σ at the cavity surface:

$$\sigma = \int_{\infty}^{a} \frac{d\sigma_r}{dr}\, dr = -\frac{4}{3} E_2 a^3 \int_{\infty}^{k} \frac{dr}{r^4} - 2Y_2 \int_{k}^{h} \frac{dr}{r}$$

$$- \frac{4}{3} E_1 a^3 \int_{h}^{b} \frac{dr}{r^4} - 2Y_1 \int_{b}^{a} \frac{dr}{r} \qquad (19)$$

It is assumed that $\sigma_r \to 0$ as $r \to \infty$, and, upon evaluation of the integrals, Equation 19 reduces to

$$\sigma = 2Y_1 \ln \frac{b}{a} + \frac{4}{9} E_1 \left(\frac{a^3}{b^3} - \frac{a^3}{h^3} \right) + 2Y_2 \ln \frac{k}{h} + \frac{4}{9} E_2 \frac{a^3}{k^3} \qquad (20)$$

SPHERICAL CAVITY EXPANSION IN A VERTICALLY LAYERED MEDIUM

Consider an infinite medium composed of two distinct vertical layers separated by a plane interface (Figure 4). A slowly

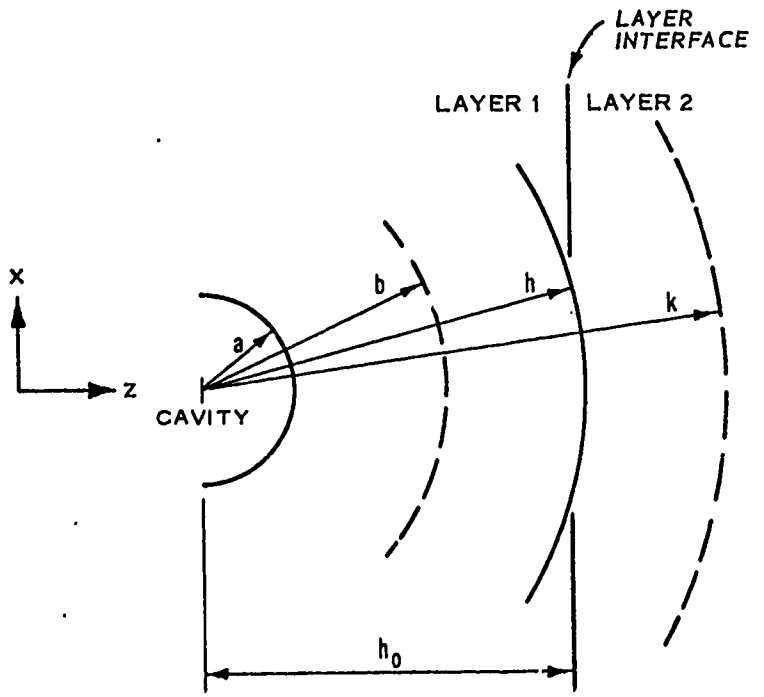

Figure 4. Slowly expanding spherical cavity in a vertically layered medium

expanding spherical cavity is centered on the z-axis at a distance h_o from the left side of the layer interface. A first-order approximation for the radial stress σ on the right hemisphere of the cavity surface can be obtained by regarding the vertical layers as quasi-concentric layers with the initial position of the layer interface located at a radial distance $r = h_o$ from the center of the cavity. The effective radial position of the layer interface is then given by Equation 18, and the first-order approximation for σ is given by Equation 20.

PROJECTILE EQUATION OF MOTION IN A VERTICALLY LAYERED MEDIUM

Projectile penetration and spherical cavity expansion represent geometrically dissimilar processes. Nevertheless it has been observed that the axial force which opposes penetration is more or less proportional to σ at low velocities in materials which are composed of a single semi-infinite layer (4,5). It has been further observed that the relation between final depth and impact velocity is approximately linear for deep penetration (5), which implies a possible linear relation between the axial resisting force and the projectile velocity. These observations will now be used as guidelines in the formulation of an *ad hoc* expression for the effective stress normal to the frontal surface of a penetrating projectile.

Consider a rigid axisymmetric projectile which penetrates a semi-infinite target composed of two distinct vertical layers (Figures 5 and 6). The projectile axis of symmetry coincides with the direction of motion, which is normal to the target surface. The quantity σ contains the pertinent dimensions and material properties of the target

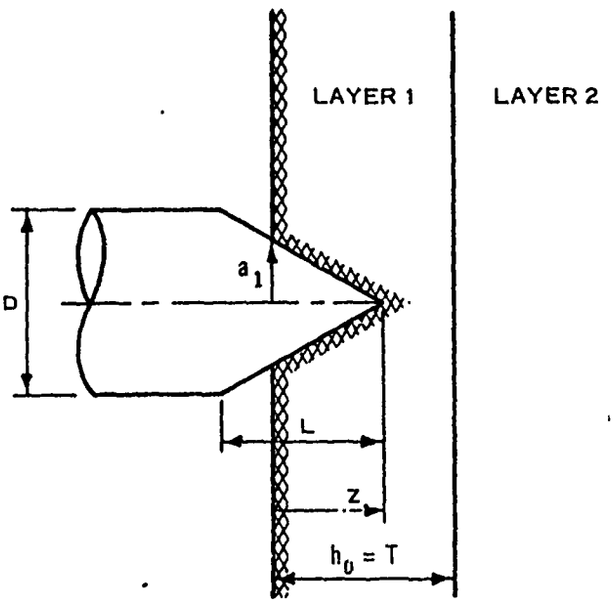

Figure 5. Projectile with frontal surface partially embedded in a two-layer target

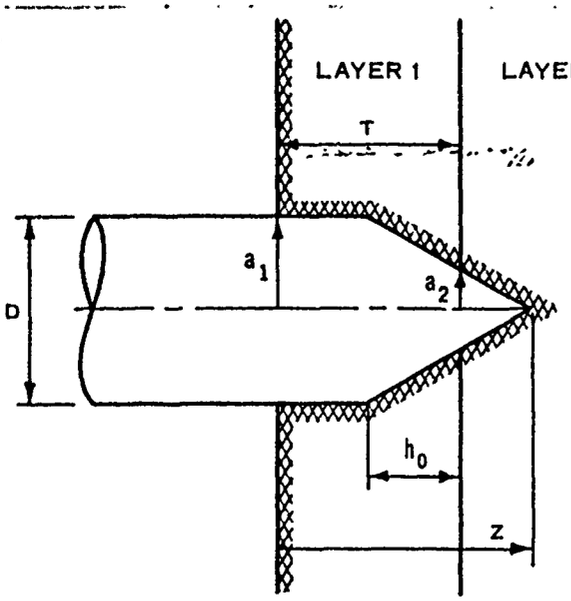

Figure 6. Projectile with frontal surface in contact with both target layers at the same time

as they relate to spherical cavity expansion, and this quantity will be used as a scaling function in the determination of the axial force which opposes the motion of the projectile.

Denoting the projectile velocity by v and the target density by ρ, the following ad hoc expression is proposed for the effective stress $\sigma_n(1)$ normal to any portion of the projectile frontal surface which is in contact with layer 1:

$$\sigma_n(1) = (1 + \sin \alpha)\sigma_1 + v\sqrt{\rho_1 \sigma_1} \qquad (21)$$

The subscripts 1 and 2 are used to designate the evaluation of quantities in layers 1 and 2, respectively. For conical nose shapes, the quantity α represents the cone half-angle, which is related to the nose length L and the base diameter D by

$$\sin \alpha = \left(\frac{4L^2}{D^2} + 1\right)^{-1/2} \qquad (22)$$

For ogival nose shapes, α represents the cone half-angle at the nose tip, which is related to the ogive caliber radius (CRH) and to L and D by

$$\sin \alpha = \frac{(4CRH - 1)^{1/2}}{2CRH} = \frac{4L/D}{4L^2/D^2 + 1} \qquad (23)$$

The evaluation of σ_1 by equation 20 is the same as the evaluation of σ for an equivalent spherical cavity with a radius equal to the maximum radius of contact a_1 between the projectile and layer 1 (Figure 5). When the frontal surface is only partially embedded in

the target, the equivalent spherical cavity is centered at the target surface, i.e.

$$h_o = T \ , \quad z \leq L \tag{24}$$

where T is the thickness of layer 1 and z is the penetration depth. When the frontal surface is fully embedded in the target, the equivalent spherical cavity is centered at the base of the nose, i.e.

$$h_o = T - z + L \ , \quad L \leq z \leq T + L \tag{25}$$

The evaluation of b , k , and h is the same as in Equations 14-18 with $a = a_1$.

In accordance with Equation 21, the effective stress $\sigma_n(2)$ normal to any portion of the frontal surface which is in contact with layer 2 is

$$\sigma_n(2) = (1 + \sin \alpha)\sigma_2 + v\sqrt{\rho_2 \sigma_2} \tag{26}$$

The evaluation of σ_2 is the same as the evaluation of σ for an equivalent spherical cavity with a radius equal to the maximum radius of contact a_2 between the projectile and layer 2 (Figure 6). This equivalent cavity is centered at the layer interface ($h_o = 0$), and Equation 20 reduces to

$$\sigma_2 = \frac{2}{3} Y_2 \left(1 + \ln \frac{2E_2}{3Y_2}\right) \tag{27}$$

Tangential stresses are neglected, and the axial component of the effective normal stress is integrated over the embedded portion of the frontal surface. The projectile equation of motion then becomes:

$$m \frac{dv}{dt} = -\pi a_1^2 \sigma_n(1) \ , \quad z \leq T \tag{28}$$

$$m \frac{dv}{dt} = -\pi \left(a_1^2 - a_2^2\right)\sigma_n(1) - \pi a_2^2 \sigma_n(2) \ , \quad T \leq z \leq T + L \tag{29}$$

$$m \frac{dv}{dt} = -\pi a_2^2 \sigma_n(2) \ , \quad z \geq T + L \tag{30}$$

where m is the projectile mass and t is time. The right-hand side of the equation of motion represents the total axial force

exerted on the projectile by the target.

Whenever the condition $\sigma_n(2) \geq \sigma_n(1)$ is satisfied, the material in layer 1 undergoes contained plastic flow, and Equation 21 represents a reasonable approximation for $\sigma_n(1)$. However, if this condition is not satisfied, then the containment provided by layer 2 may be insufficient to prevent a loss of cohesion in layer 1, and Equation 21 then represents an upper bound for the value of $\sigma_n(1)$. In this event, a lower bound can be obtained for $\sigma_n(1)$ by introducing the following "plastic interface criterion:"

If $\sigma_n(2) < \sigma_n(1)$ when $b = h$ (i.e. when the spherical plastic front located at $r = b$ reaches the effective layer interface located at $r = h$), then Equation 21 is replaced by

$$\sigma_n(1) \approx \sigma_n(2) = (1 + \sin \alpha)\sigma_2 + v\sqrt{\rho_2 \sigma_2} \qquad (31)$$

PENETRATION AND PERFORATION OF CONCRETE SLABS

Canfield and Clator (6) have investigated the high speed penetration of steel projectiles into thick slabs of 5000-psi reinforced concrete, and their experimental results are shown in Figure 7. The projectile characteristics are $m = 5.9$ kg, $D = 76.2$ mm, and $CRH = 1.5$ (ogival nose shape, $L/D = 1.12$). The target properties are $\rho = 2.31$ gm/cm^3, $E = 240$ kbar, and $Y = 0.347$ kbar. The projectile equation of motion developed in the present work is integrated to obtain the theoretical relation between final depth and impact velocity (Figure 7), based on the assumption of a single semi-infinite layer of homogeneous concrete. The empirical results shown in Figure 7 are obtained from a penetration nomogram for concrete developed by the National Research Council (NRC) committee on passive protection against bombing (7). The NRC nomogram is allegedly accurate to within 15 percent, and the agreement achieved among the empirical, experimental, and theoretical results is typical for cohesive targets in which the distance from the nose tip to the back face of the target is large in comparison with the projectile diameter ($T - z \gg D$).

The results shown in Figure 7 provide partial verification of the applicability of the theory for cohesive targets composed of a single semi-infinite layer. Now, in order to make an assessment of the applicability for targets composed of distinct layers, the theory is used to calculate the penetration and perforation of a concrete slab of finite thickness. This represents an example of a

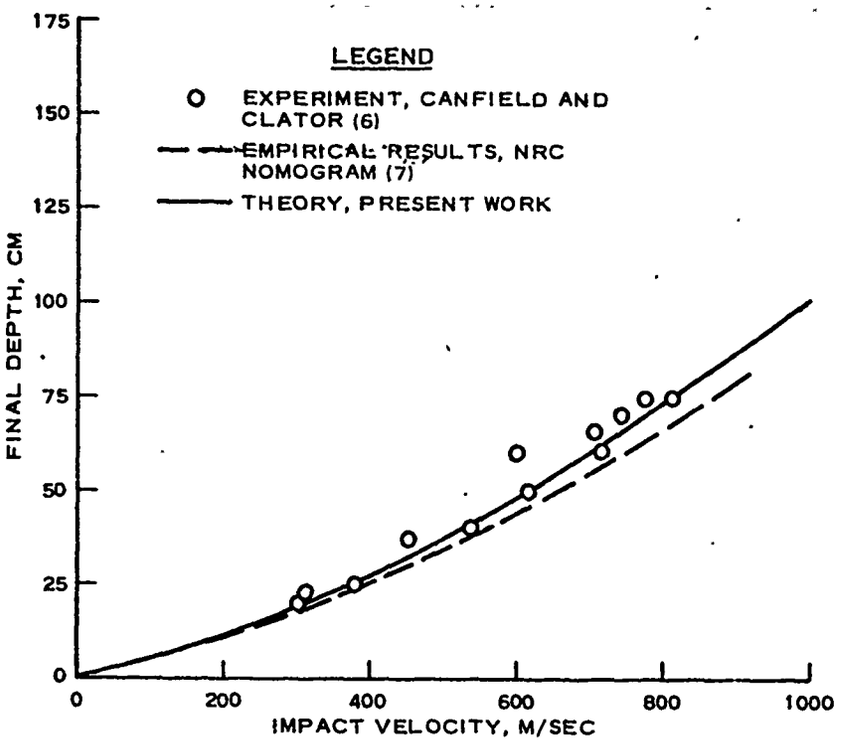

Figure 7. Penetration performance of 76-mm steel projectile in a semi-infinite slab of 5000-psi concrete

two-layer configuration in which the first layer (concrete) has a finite strength and density while the second layer (air or vacuum) has a negligible strength and density. The concrete properties and the projectile characteristics are identical with those used in the foregoing calculation for a semi-infinite concrete slab, but in the present calculation the projectile equation of motion is integrated numerically to determine the minimum impact velocity required for complete perforation* of a slab with a given finite thickness. The theoretical results are compared with empirical results in Figure 8. The empirical results are obtained from an NRC perforation nomogram for concrete slabs (7) which is allegedly accurate to within 15 percent.

Two sets of theoretical results are presented in Figure 8,

* Complete perforation means that the projectile frontal surface passes completely through the slab, achieving a penetration depth $z \geq T + L$ (Figures 5 and 6).

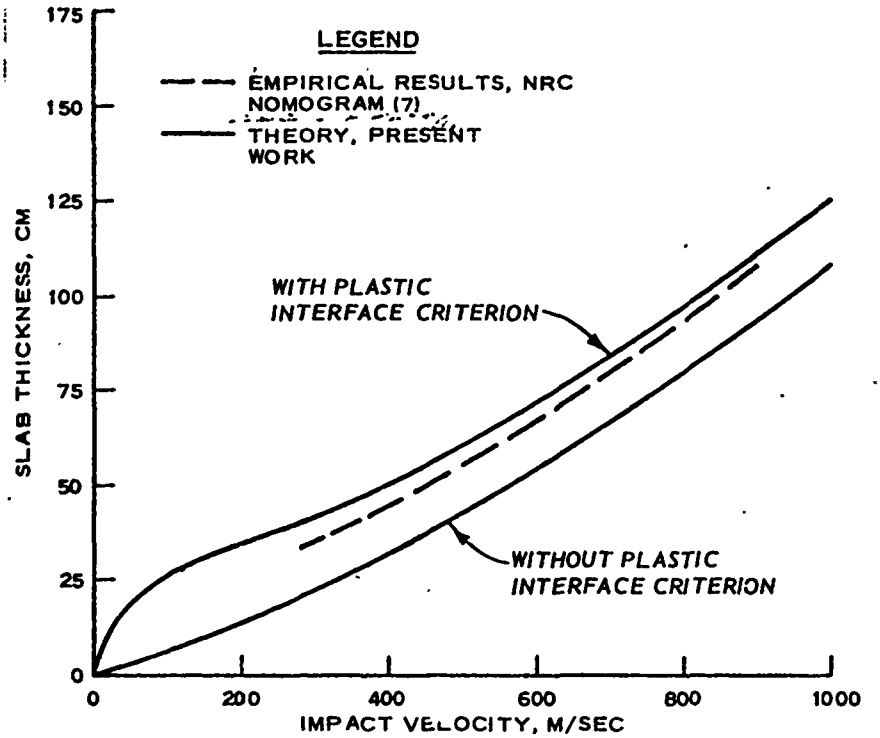

Figure 8. Minimum thickness of 5000-psi concrete required to prevent complete perforation by a 76-mm steel projectile

corresponding to calculations made with and without the plastic interface criterion (Equation 31). The theoretical results form a fairly tight band about the empirical results, but the calculations made with the plastic interface criterion produce the best agreement with the NRC nomogram. The end points of the empirical curve coincide with the ranges of impact velocity and slab thickness for which the nomogram is applicable.

CONCLUSION

The projectile equation of motion which has been developed herein appears to be applicable for cohesive slabs and layered targets in which the thickness of a given slab or layer is greater than the projectile base diameter by at least a factor of five. The spherical cavity expansion analysis, which is used as the basis of the penetration theory, is inappropriate when the diameter of the projectile is comparable with the dimensions of the target. The analysis of the penetration of thin target layers ($T \lesssim D$) requires

a different conceptual approach which lies beyond the scope of the present work. The theory can be used to calculate the instantaneous deceleration, velocity, and position of a rigid cylindrical projectile (with conical or ogival nose shape) when the direction of motion is coincident with the projectile axis of symmetry and normal to the target surface. The details of the target motion are not predicted by the theory, which relies on a highly idealized model of the projectile/target interaction. Two-dimensional finite-difference solutions represent the only means presently available for assessing the details of the target behavior during the penetration process.

REFERENCES

1. B. Robins, New Principles of Gunnery, London, 1742.

2. L. Euler, Neue Grundsätze der Artillerie, Berlin; reprinted as Euler's Opera Omnia, Druck und Verlag von B. G. Teubner, Berlin, 1922, first edition, p. 450.

3. J. V. Poncelet, Cours de Mécanique Industrielle, 1829, first edition.

4. R. F. Bishop, R. Hill, and N. F. Mott, "The Theory of Indentation and Hardness Tests," Proceedings, London Physical Society, Vol 57, 1945, pp. 147-159.

5. J. N. Goodier, "On the Mechanics of Indentation and Cratering in Solid Targets of Strain-Hardening Metal by Impact of Hard and Soft Spheres," Proceedings, Seventh Hypervelocity Impact Symposium, Vol III, Tampa, Fla., Feb 1965, pp. 215-260.

6. J. A. Canfield and I. G. Clator, "Development of a Scaling Law and Techniques to Investigate Penetration in Concrete," NWL Report No. 2057, U. S. Naval Weapons Laboratory, Dahlgren, Va., Aug 1966.

7. "Terminal Ballistics and Explosive Effects," National Research Council, Committee on Passive Protection against Bombing, Washington, D. C., Oct 1943.

ACKNOWLEDGMENTS

This work was sponsored by the Defense Nuclear Agency under Subtask SB211, Work Unit 09, "Earth Penetrator Calculation Studies and Comparative Analysis with Field Measurements." The application of the cavity expansion analysis to the projectile penetration problem for layered targets was originally suggested by Professor S. V. Hanagud, Georgia Institute of Technology, Atlanta, Georgia.